SWE Reanalysis Model Temperature Threshold Sensitivity Analysis in the Olympic Mountains

Hannah Besso, Carina Thompson, Eric Gagliano
CEE 568: Snow Hydrology
March 19, 2021

Github Repository: https://github.com/bessoh2/SnowHydro

Abstract

We analyzed the ability of the Particle Batch Smoother (PBS) Reanalysis model to estimate snow water equivalent (SWE) over the Olympic Mountains and compared model outputs that used three different temperature thresholds for precipitation partitioning. The goal of this study was to determine model sensitivity to the temperature threshold parameter and to develop a recommendation for the use of regional as opposed to continental thresholds. We compared the PBS model SWE output to airborne lidar-derived SWE data over the same set of days, masked out glaciers, and differenced the SWE maps. We show that there is strong agreement between the PBS output and the ASO data at the 0℃ threshold. A regression analysis confirms the strong agreement between model and ground truth that increases in strength as we step from the 2℃ temperature threshold to 1℃ and 0℃. This change in precipitation temperature partitioning threshold correlates to an approximately 10% increase in accuracy from the original 2℃ threshold to the updated 0℃ threshold. Our results show that the PBS model is sensitive to the temperature threshold, and that threshold choices above 0℃ lead to an overestimation of regional SWE. Accordingly, we recommend that the PBS model should regionalize the temperature threshold for precipitation partitioning in order to improve SWE estimation.

1 Introduction

1.1 Study Purpose

Snow provides a significant source of water to approximately ⅙ of the world's population (Barnett et al. 2005). It provides a natural reservoir of water that can sustain river discharges during dry summer months. Despite the importance of snow for maintaining irrigation, drinking water, and numerous ecological benefits throughout the melt season, we still lack in-situ snow measurements at a representative spatial scale. Remote sensing has proven to be a valuable tool for measuring snow depth, but due to a lack of high spatial and temporal resolution, remote sensing is often combined with snow modeling to estimate basin snow water equivalent (SWE).

One such model is a new SWE Reanalysis Particle Batch Smoother (PBS) model, recently developed by the Margulis lab at UCLA. This new model has a spatial resolution of 500 m and covers the entire continental US, but has yet to be rigorously validated. A model using similar methods with higher spatial resolution (90 m) but lower spatial extent, also developed by the Margulis lab, was shown to have high accuracy in the Sierra Nevadas with RMSE values on the order of centimeters (Margulis et. al., 2016). Therefore, this new continental-scale SWE

Reanalysis model is promising, but is still undergoing validation. Due to the greater spatial extent of this model, the input parameters are also coarser, and a number of generalizing assumptions are made. One of these assumptions is the use of one single temperature threshold for the partitioning of rain and snow across the entire continental US. Based on previous literature (Currier et. al., Jennings et. al., Sun et. al., etc) we know that rain/snow temperature thresholds vary spatially across the US, and so we hypothesize that using one constant threshold for the entire model extent may be contributing to errors in SWE estimation. To investigate this further and to provide recommendations for model improvement, we aimed to compare model accuracy using model outputs that were run using a variety of temperature threshold values. This analysis was focused on the Olympic Mountains of Washington State because of the differences in meteorologic conditions (such as a greater amount of cloud cover) that exist in the Olympics as compared to the continental and intercontinental mountain ranges in the US. This study sought to inform future use of this new model in coastal mountain regions and to provide the model developers with recommendations for future model improvements.

1.2 Temperature Threshold

Temperature thresholds used in snow modeling for partitioning precipitation between rain and snow can have a large impact on snow accumulation, especially in regions that tend to hover right around that temperature threshold during precipitation events. The temperature threshold depends primarily on relative humidity and pressure, and therefore varies across regions with different meteorologic conditions. Despite this known variation in temperature thresholds across different regions, the continental-scale SWE Reanalysis PBS model uses a constant threshold across the entire United States of approximately 2℃. Based on previous temperature threshold studies in the Olympics (Currier et al., 2017 & Jennings et al., 2018), we expect a threshold of approximately 0℃ would most accurately partition between rain and snow at this site. Another study (Sun et. al., 2018) found the 50% threshold between rain and snow to be approximately 1℃ in the Cascade Mountains of Washington State, which fall within the same general region as the Olympic Mountains.

Therefore, with the gracious help of researchers at the Margulis lab, we decided to test whether we saw model improvement in the Olympics using these different temperature thresholds. Yiwen Liu, a PhD student working with Dr. Margulis, agreed to help by rerunning the model over the Olympics at additional temperature thresholds of 0℃ and 1℃. With these additional model runs, we aimed to compare model accuracy between threshold values. Our analysis hoped to determine the sensitivity of the model to the threshold temperature, and to inform the Margulis lab on changes in model accuracy obtained by using regionalized temperature thresholds as opposed to a constant continental threshold.

1.2 Study Area Description

The Olympic Mountains are located on the Olympic Peninsula in Washington State, and are classified as a temperate rainforest. They are characterized by large amounts of precipitation, moderate temperatures, and frequent cloud cover. This makes them unique to most other ranges in the United States, with the Cascade Mountains being the most similar range. The Olympic Mountains have a lower temperature threshold than most other ranges in the country (Jennings et. al., 2018 and Sun et. al., 2019) and therefore provide an opportunity to test the effects of different temperature thresholds used by the SWE Reanalysis PBS model. High resolution airborne lidar was flown over the range in 2016 as part of the Olympex campaign, which provides a high accuracy SWE dataset for comparison with the model outputs (Figure 1).

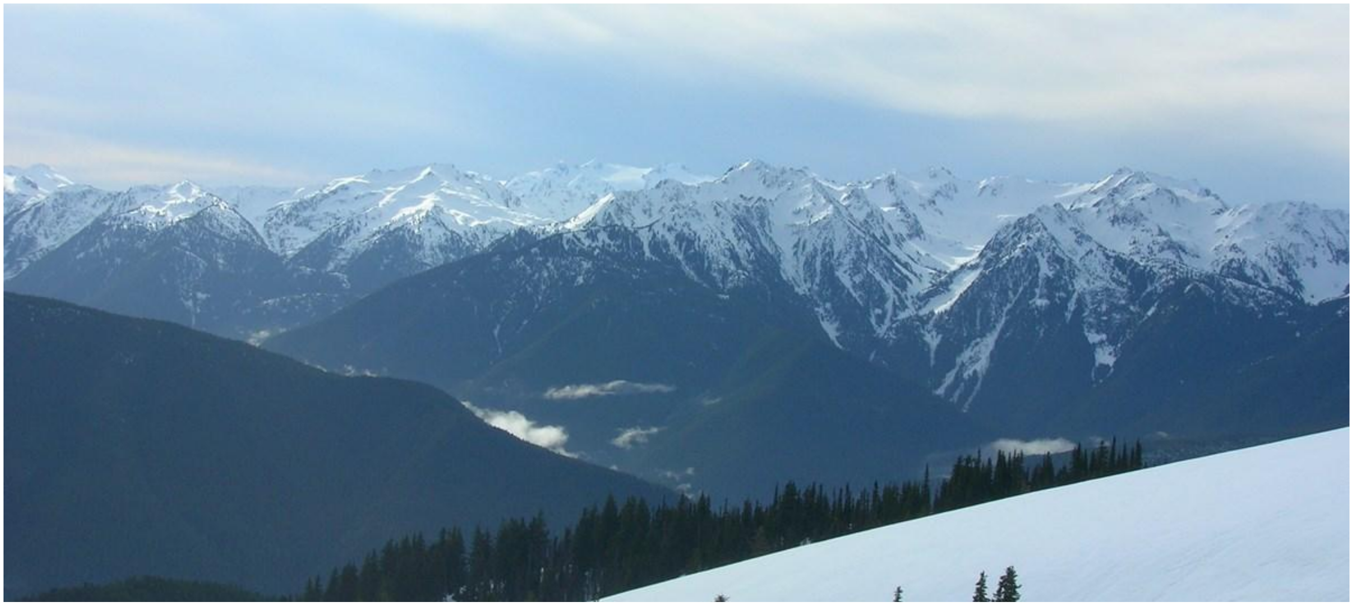

Figure 1. The Olympic Mountains, taken from Hurricane Ridge (courtesy of the US NPS).

1.3 Datasets

The Particle Batch Smoother (Margulis et al, 2015) is a fairly new and promising method for SWE reanalysis. Previous SWE Reanalysis model approaches applied a Kalman Ensemble Batch Smoother, whereas this Particle Batch Smoother approach has the advantage of more heavily weighting model parameters that closely match SWE observations. As a result, the Particle Batch Smoother approach's generality leads to overall improvement in SWE reanalysis by more effectively removing prior biases and better constraining high input uncertainties. The PBS method was implemented in a high resolution (90 m) SWE Reanalysis model that was run over the Sierra Nevadas with high accuracy, as mentioned earlier (Margulis et. al., 2016). A new product using this same method at coarser resolution (500 m) is under development by the Margulis lab at UCLA. It uses meteorological input data from the National Center for Environmental Prediction (NCEP) as well as certain parameter assumptions, including rain vs snow temperature partitioning, to quantify SWE over a given region. Preliminary model output for the original model and additional runs using a variety of temperature thresholds were provided via personal correspondence by members of the Margulis Lab.

To validate the model output, we used high resolution, high accuracy aerial lidar from the Airborne Snow Observatory (ASO) (Painter et. al., 2016). This aerial lidar was obtained over the Olympic Mountains on two dates in 2016: February 8 and March 29. This SWE data was downloaded from the National Snow and Ice Data Center (NSIDC) at a spatial resolution of 50 m, and served as the ground truth to which we compared the model output.

2. Methods

2.1 Preprocessing

In order to directly compare the ASO lidar data to the model output, we upscaled the lidar-derived snow depth data from 50 meter resolution to 500 meter resolution. We did this in Python using the open-source package rasterio, and used the bilinear interpolation method. Next, we cropped the northern extent of the aerial lidar data to that of the model output, and then used the rasterio reproject match function to project the model output data and match it's spatial extent to that of the aerial lidar. Based on personal correspondence with the Margulis lab at UCLA and the Lundquist lab at UW, we determined that glaciers in the Olympic Mountains were a source of error for both datasets. Therefore we decided to mask out all pixels that contained glaciers. To do this, we downloaded glacier polygons from the Global Land Ice Measurements from Space (GLIMS) and used these to clip the model output. We chose to clip out any pixel that contained any amount of glacier, instead of setting a glacier area threshold for clipping (Figure 2). This was the most conservative route, and we decided that excluding all glacial areas would yield the most accurate results. This preprocessing was repeated for the model outputs obtained from using a temperature threshold of 0℃, 1℃, and 2℃.

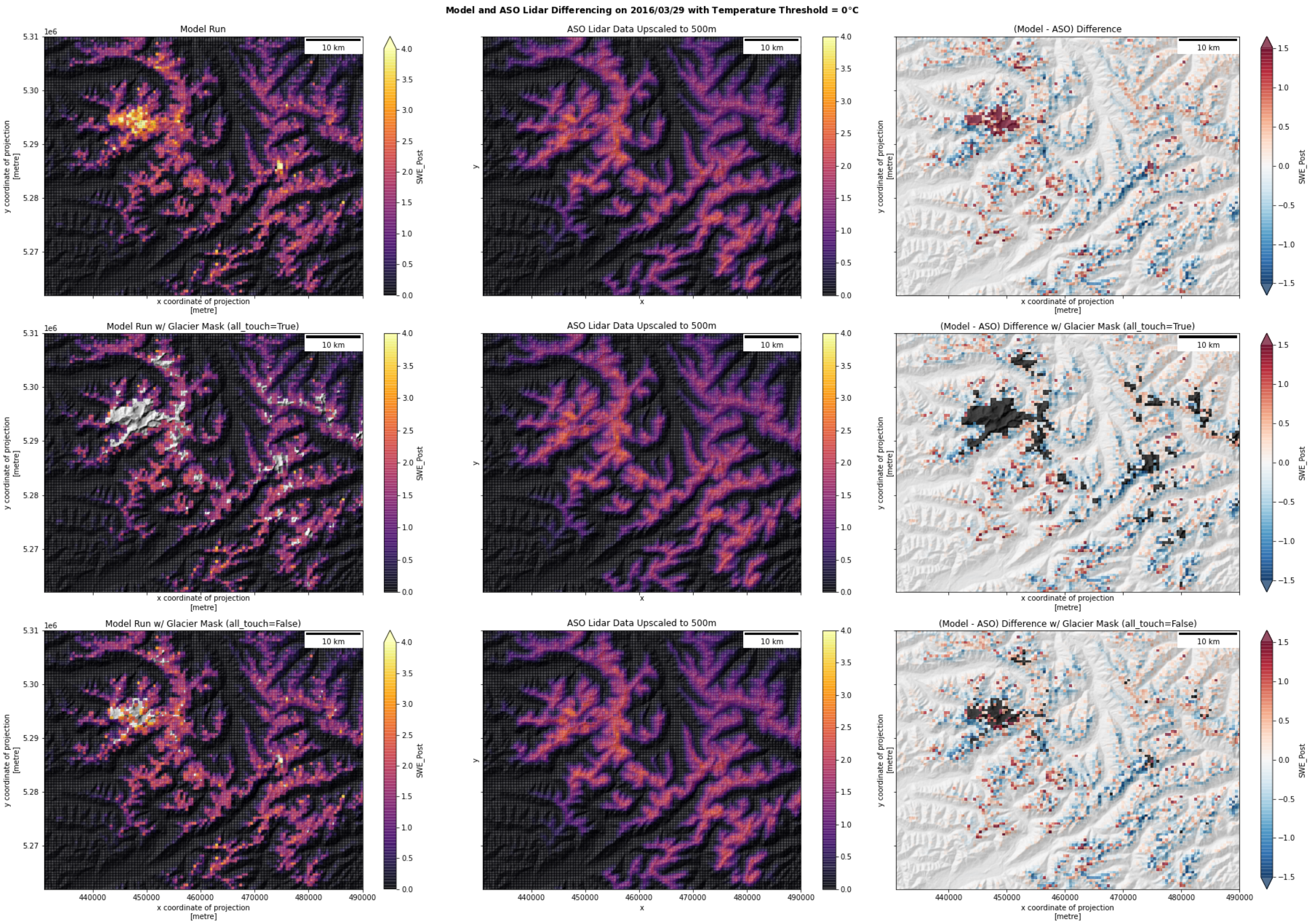

Figure 2. Model runs (left), ASO lidar data (middle) and differenced SWE (right) for a variety of glacier masking options: no mask (top), all pixels containing glaciers masked (middle) and pixels with over 50% glacier by area masked (bottom). We chose to proceed by masking out all pixels containing glaciers (middle).

2.2 Data Analysis

To determine the accuracy of the modeled output, we subtracted the aerial lidar from the model output for all three temperature thresholds. This resulted in rasters with model error values. From these rasters, we computed the mean and standard deviation of the differences between the data sources. We also conducted a linear regression to determine the correlation between the aerial lidar and model output datasets. Finally, we compared these results to determine the temperature threshold that yielded the most accurate snow water equivalent model output.

3. Results

3.1 Differencing Aerial Lidar SWE from Modeled SWE

After differencing across all temperature thresholds and day combinations, we noticed strong agreement between the model output and the ASO data. As noted earlier, masking out the pixels with glaciers was essential to identifying this strong agreement between the model and the ground truth. Of particular importance were mean differences close to 0 with relatively small standard deviations across all model runs. We note that these two metrics seem to deviate from strong agreement to moderate agreement with the aerial lidar data as we step from the 0℃ temperature threshold to 1℃ and 2℃, as well as from 2016/03/29 to 2016/02/08. We can quantify this change in agreement: the resulting accuracy ranged from a mean difference for 2016/03/29 at the 0℃ temperature threshold of -0.028m with a standard deviation of 0.303m, to a mean difference for 2016/02/08 at the 2℃ threshold of 0.127m with a standard deviation of 0.324m (Figure 3).

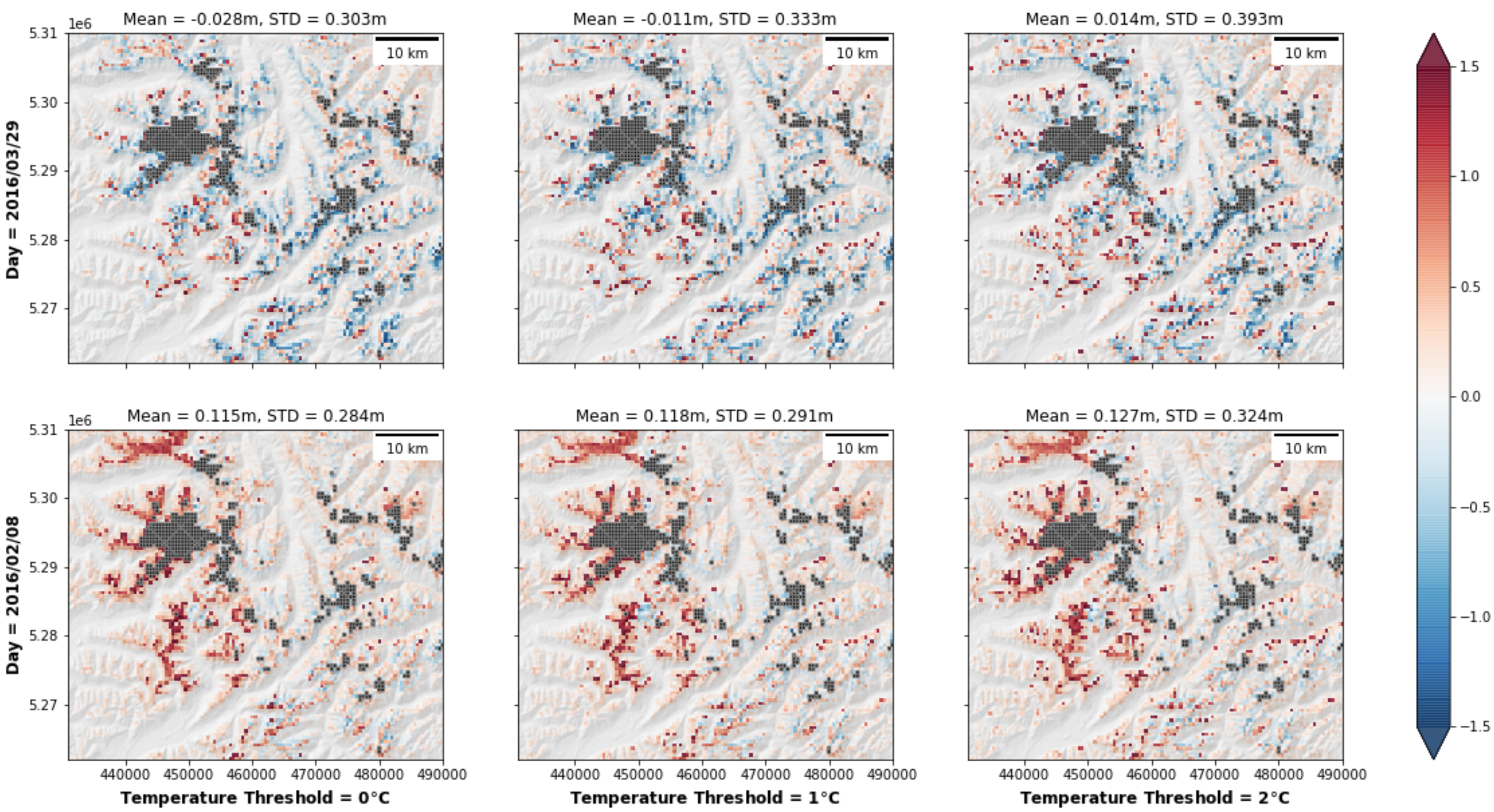

Figure 3. Differences between the ASO lidar SWE and the modeled SWE. Red pixels indicate overestimation of SWE by the model, blue represent underestimation of SWE, and the closer the colors are to white indicate agreement between the model and the ASO data. From left to right, the plots show results for the model runs with a temperature threshold at 0℃, 1℃, and 2℃ respectively. The top plots show model runs for March 29, 2016 and the bottom plots show results for February 8, 2016.

3.2 Difference Histograms

There was a positive skew in the distributions of all of the model runs, with the most severe skews appearing at 2016/02/08 (Figure 4). This larger distribution of positive pixel differences means the model overestimated SWE for both days and for all temperature thresholds. There appears to be a higher concentration of red pixels (indicating model overestimation) at higher elevations for all runs, as well as a greater number of red pixels for runs on February 8 than for those on March 29.

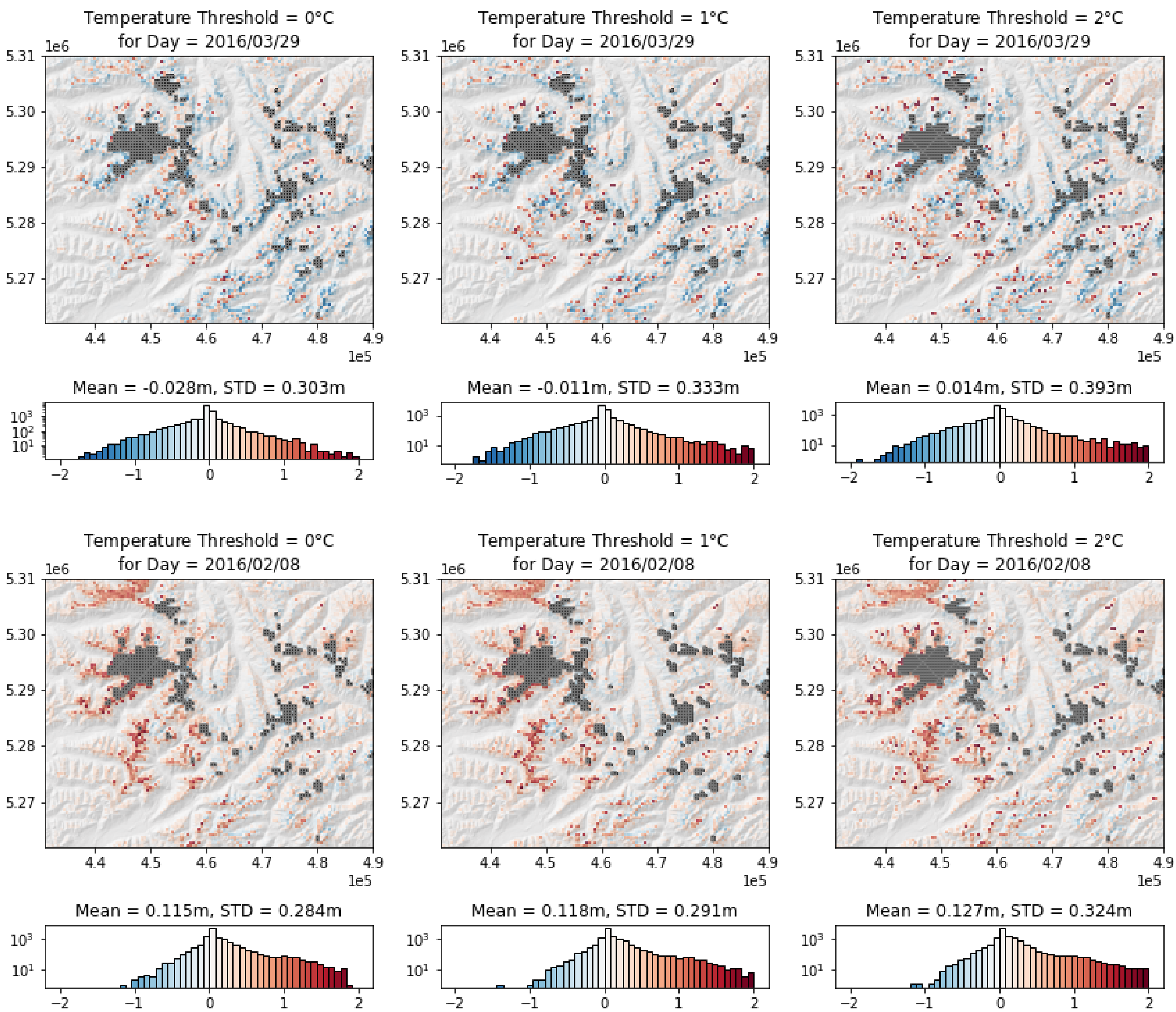

Figure 4. Below each difference plot is the image histogram. This helps us visualize both the spatial distribution of difference values as well as the numerical distribution of the difference values. Note that the color gradient between the histograms and the difference plots is the same.

3.3 Regression Analysis

Finally, the regression analysis quantitatively confirms the strong agreement between model and ground truth that decreases in strength as we step from the 0℃ temperature threshold to 1℃ and 2℃, as well as from 2016/03/29 to 2016/02/08 as noted earlier (Figure 5). This can be seen in our range of R^2values, which represent the amount of variance the regression model explains. For example, the range of R^2 values extends from a strong R^2 = 0.854 for 2016/03/29 at the 0℃ threshold, to a weaker R^2 = 0.398 for 2016/02/08 at the 2℃ threshold. We can visualize these differences in Table 1. We will talk more about the implications of these values in the following discussion.

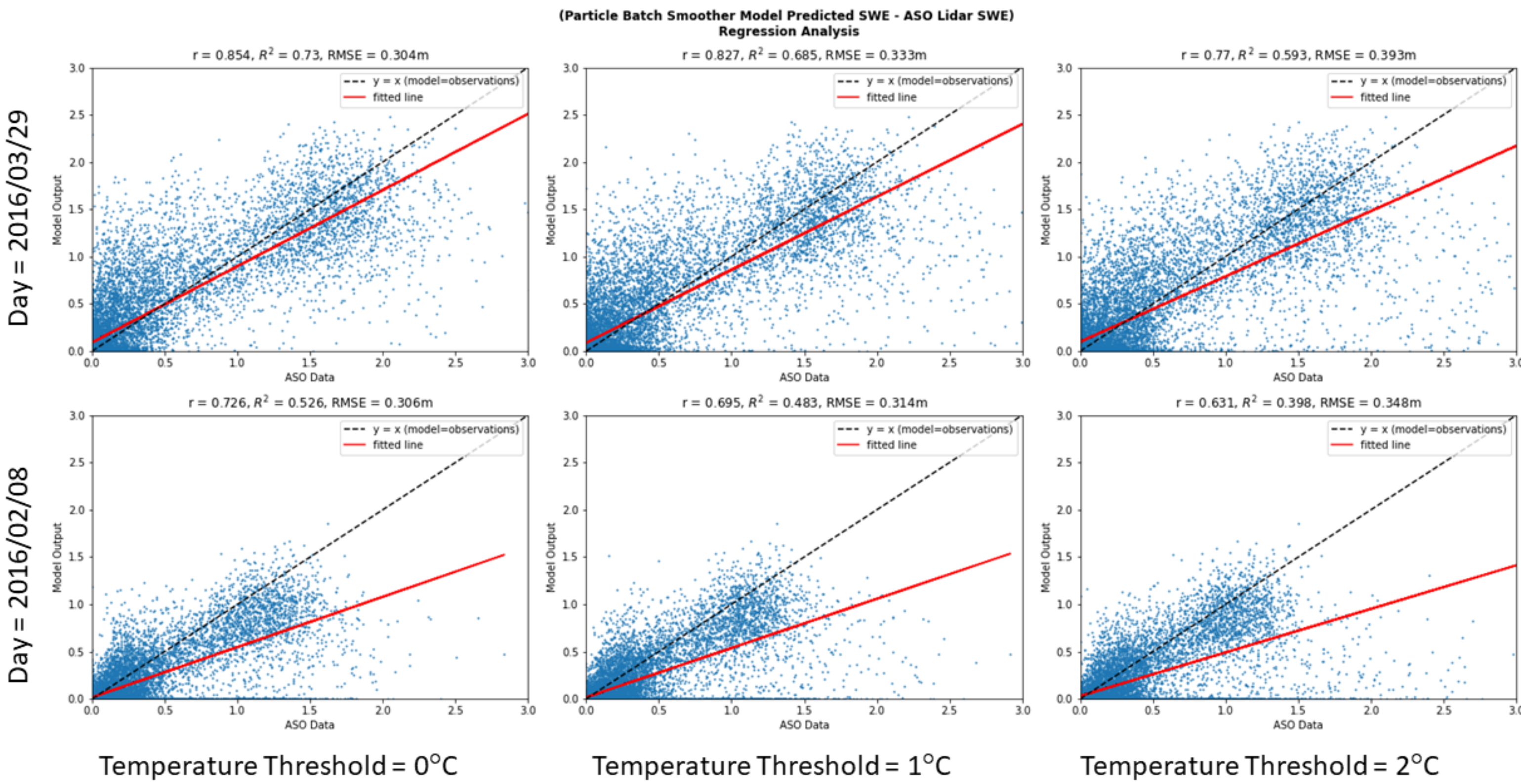

Figure 5. Regression analysis for all temperature threshold and day combinations. Note that the r, R^2, and RMSE given above each plot.

RMSE (m)				
		Temperature Threshold in degrees Celsius		
		0	1	2
Day (in 2016)	03/29	0.304	0.333	0.393
	02/08	0.306	0.314	0.348

R^2				
		Temperature Threshold in degrees Celsius		
		0	1	2
Day (in 2016)	03/29	0.73	0.685	0.593
	02/08	0.526	0.483	0.398

Table 1. RMSE and R^2 values given for all temperature threshold and day combinations. To highlight differences, green indicates a more preferable parameter value (lower RMSE, higher R^2), while red indicates a less preferable parameter value (higher RMSE, lower R^2).

4. Discussion

Overall, the modeled SWE showed strong agreement with the aerial lidar-derived SWE values. Between model runs, accuracy increased from the higher to lower temperature threshold values, with the highest accuracy resulting from the 0℃ threshold. This was consistent with previous literature mapping the spatial distribution of rain versus snow partitioning temperatures in the Pacific Northwest and the Olympic Mountains (Jennings et. al., 2018, Sun et. al., 2019). The R values for March 29 and February 8 increased by 8.4% and 9.5%, respectively from the 2℃ to 0℃ threshold model runs. This is almost a 10% increase in accuracy obtained by updating the temperature threshold parameter to a regionalized value, and shows that this SWE Reanalysis PBS model is fairly sensitive to this parameter.

There was higher accuracy across all temperature thresholds for the model runs on March 29 than for those on February 8. This may be due to different meteorologic conditions on those specific days. For example, cloud cover on the February date could have caused errors in satellite data used in the model. Clouds would impact the longwave radiation calculations as well, which the model might not be able to capture as accurately as clear sky conditions. There may be other reasons for this difference in accuracy between days, and for future analyses we would discuss these results with the model developers and would analyze meteorologic conditions on those days to determine model-specific methods that could impact accuracy day-to-day.

From a visual inspection of the spatial distribution of the differences, we noticed that there are greater concentrations of positive differences (model overestimations of SWE) at higher elevations. It is unclear whether this is due to model-specific parameterization of elevation values, or whether this is due to differences in vegetation cover at lower versus higher elevations in the Olympics. Further analysis is needed to determine the cause(s) of the model's apparent overestimation at higher elevations.

5. Conclusion

Based on the comparison between aerial lidar and the SWE Reanalysis PBS model data, a regional temperature threshold of 0℃ yields the most accurate SWE estimates over the Olympic Mountains. This is an increase in accuracy of almost 10% as compared to the original model run using 2℃ as a temperature threshold. Based on these results, we highly recommend future efforts to regionalize temperature thresholds in the SWE Reanalysis PBS model. Additionally, due to the large errors in glaciated regions that we found in our preliminary work over the Olympics, further efforts to adequately mask out additional glaciated regions outside of the Olympic Mountains may improve model results in other regions. A parameter we did not look into that we believe has the potential to impact model accuracy, especially in the Olympic Mountains, is vegetation type and cover. We recommend that future work in understanding model sensitivities and identifying improvement methods should focus on quantifying differences in SWE accuracy between different amounts of canopy cover, since vegetation is often a source of error for aerial lidar and satellite datasets. In conclusion, we recommend regionalizing the temperature threshold value for this model, and anticipate that the results of this study will motivate further analysis into the use of the SWE Reanalysis PBS model. This new model has a large extent and fairly high accuracy SWE estimations, and we anticipate that it will prove extremely useful in furthering our knowledge of snow in regions previously lacking accurate SWE estimates.

6. Acknowledgements

This work would not have been possible without the help from the Margulis lab at UCLA, especially Yiwen Liu who provided us with various model runs to complete our performance analysis. Additionally, we would like to send thanks to Dr. Jessica Lundquist, Dr. Nicoleta Cristea, and Dr. Ryan Currier whose work and guidance enabled us to complete work and contribute to this area of study.

References

Sun, N., Yan, H., Wigmosta, M. S.,Leung, L. R., Skaggs, R., & Hou, Z.(2019). Regional snow parameters estimation for large‐domain hydrological applications in thewestern United States.Journal ofGeophysical Research: Atmospheres,124, 5296–5313. https://doi.org/10.1029/2018JD030140

Margulis, S. A., Cortés, G., Girotto, M., & Durand, M. (2016). A Landsat-Era Sierra Nevada Snow Reanalysis (1985–2015), *Journal of Hydrometeorology*, *17*(4), 1203-1221. Retrieved Mar 9, 2021, from https://journals.ametsoc.org/view/journals/hydr/17/4/jhm-d-15-0177_1.xml

Margulis, S. A., Girotto, M., Cortés, G., & Durand, M. (2015). A Particle Batch Smoother Approach to Snow Water Equivalent Estimation, *Journal of Hydrometeorology*, *16*(4), 1752-1772. Retrieved Mar 9, 2021, from https://journals.ametsoc.org/view/journals/hydr/16/4/jhm-d-14-0177_1.xml

Jennings, K.S., Winchell, T.S., Livneh, B. *et al.* Spatial variation of the rain–snow temperature threshold across the Northern Hemisphere. *Nat Commun* **9,** 1148 (2018). https://doi.org/10.1038/s41467-018-03629-7

Thomas H. Painter, Daniel F. Berisford, Joseph W. Boardman, Kathryn J. Bormann, Jeffrey S. Deems, Frank Gehrke, Andrew Hedrick, Michael Joyce, Ross Laidlaw, Danny Marks, Chris Mattmann, Bruce McGurk, Paul Ramirez, Megan Richardson, S. McKenzie Skiles, Felix C. Seidel, Adam Winstral. The Airborne Snow Observatory: Fusion of scanning lidar, imaging spectrometer, and physically-based modeling for mapping snow water equivalent and snow albedo, Remote Sensing of Environment, Volume 184, 2016, Pages 139-152, ISSN 0034-4257, https://doi.org/10.1016/j.rse.2016.06.018.

Currier, W. R., Thorson, T., & Lundquist, J. D. (2017). Independent Evaluation of Frozen Precipitation from WRF and PRISM in the Olympic Mountains, *Journal of Hydrometeorology*, *18*(10), 2681-2703. Retrieved Mar 9, 2021, from https://journals.ametsoc.org/view/journals/hydr/18/10/jhm-d-17-0026_1.xml